ISME

Iranian Journal of Mechanical Engineering
The Iranian Society of Mechanical Engineers
Research Paper

DOI: 10.30506/JMEE.2022.550101.1284
DOR: 20.1001.1.16059727.2022.23.2.3.2

Numerical Study of Flow Field in New Design Cyclones with Different Vortex Finder Shapes

H. Safikhani[*]
Associate Professor

M. Modabberifar[†]
Associate Professor

H. Nazaripoor[‡]
Ph.D.

In this paper, the effect of vortex finder shape on the performance and flow field of the new design cyclones is numerically investigated using CFD techniques. Nine different geometries of vortex finder are studied in three categories each with three geometries. In the first category, the effect of vortex finder flattening is investigated. In the second category, vortex finders with three different cross section geometries circular, square and triangular are investigated. Finally, in the third category, circular vortex finders with three different diameters are modeled. The new design cyclone is based on the idea of improving cyclone collection efficiency and pressure drop by increasing the vortex length. The Eulerian-Lagrangian computational procedure is used to predict particles tracking in the cyclones. The velocity fluctuations are simulated using the Discrete Random Walk (DRW). The results show that in the flat category, vortex finder without flattening (circular cross section) possess the maximum efficiency and the lowest pressure drop and with flattening, the cyclone efficiency dramatically decreases while pressure drop remarkably increases. Among the vortex finder with different cross section, maximum efficiency is associated to the circular vortex finder while the lowest pressure drop is assigned to the triangle one.

Keywords: Vortex finder shape, New design cyclone, Flat tube, CFD, DRW.

1 Introduction

Cyclones are vastly applied for different purposes including air pollution control and industrial applications. Due to their favorable properties such as relative simplicity of their fabrication,

[*] Associate Professor, Department of Mechanical Engineering, Faculty of Engineering, Arak University, Arak 38156-88349, Iran, h-safikhani@araku.ac.ir
[†] Corresponding Author, Associate Professor, Department of Mechanical Engineering, Faculty of Engineering, Arak University, Arak 38156-88349, Iran, m-modabberifar@araku.ac.ir
[‡] Ph.D., Department of Mechanical Engineering, University of Alberta, Canada, hadi@ualberta.ca

Receive: 2022/03/06 Accepted: 2022/07/24

low operation cost and high compatibility with harsh condition, separating cyclones have been considered among important particle separation equipment. Starting from the Alexander [1], many researches have been investigated to improve the performance of the cyclones such as collection efficiency and pressure drop by manipulating geometrical and process parameters of the cyclone. The effect of cyclone inlet dimension on its performance was numerically studied by Elsayed and Lacor [2]. They found width of the inlet is much more influential than the height of the inlet especially for collection efficiency. Zhao et al. [3] investigated the performance of two different cyclones, one with plain single inlet and the other with spiral double inlet. Numerical results proved that novel cyclone with spiral double inlet can improve the flow field pattern culminating in separation efficiency. Impacts of the cone dimension on cyclone performance was also investigated which was shown if cone size is higher than gas outlet dimension, decreasing cone size can improve collection efficiency without increasing pressure drop [4-6]. Yoshida et al. [7] used different apex cones for cyclone inlets and reported that at high inlet velocity, the influence of the cone angle on collection efficiency decreases. The performance of a cyclone improved by a vertical pipe also was studied [8, 9]. The possible influence of the counter-cone at the bottom of the cyclones on their performance was also studied [10-12]. One of the most important parts of a cyclone that has significant impact on its performance is the Vortex Finder as highlighted in cyclone geometry in Fig. (1). The effect of the shape of vortex finder on the cyclone performance was the focus of some studies in recent years. Khalkhali and Safikhani [13], by combining CFD, neural networks and NSGA II algorithm, in a multi-objective process, optimized the shape of the vortex finder in conventional cyclones. They finally presented the Pareto front and five optimized non-dominated vortex finder shape. Raoufi et al. [14] numerically investigated the effect of different vortex finder shapes on conventional cyclone performance. They investigated the effect of divergence, convergence, diameter, fragmentation, etc. on cyclone performance.

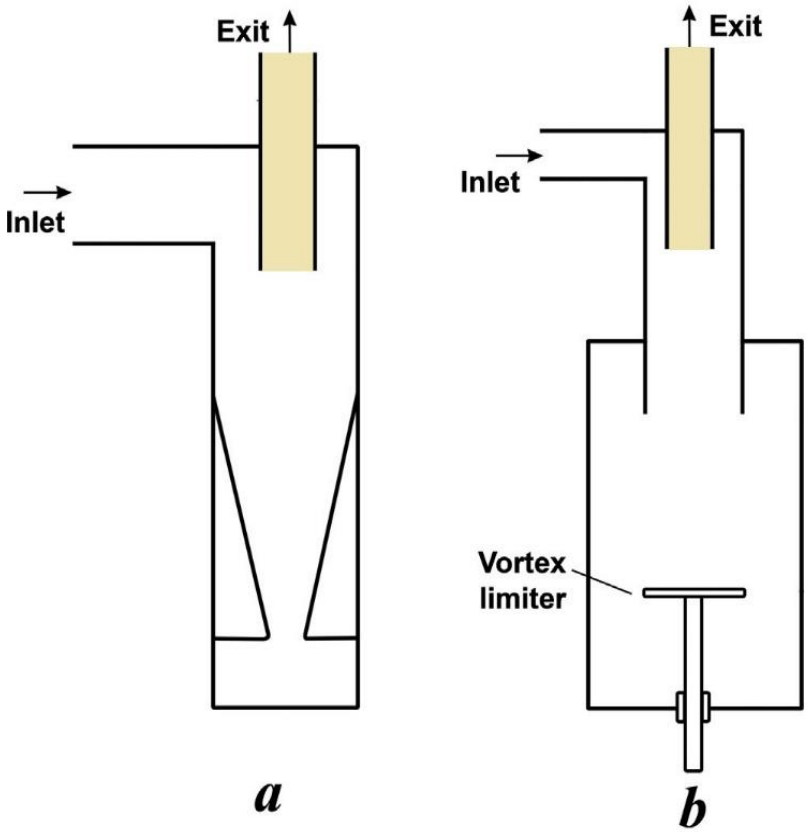

Figure 1 Schematic comparison of new cyclones and conventional ones, vortex finder part is highlighted.

Recently, considering the positive correlation between vortex length and cyclone performance, Karagoz et al. [15] proposed a new cyclone design in which instead of a cone, separation space of new cyclone is made of a cylinder with a vortex limiter. Fig. (1) compares the schematic geometry of Karagoz new design and convectional cyclones. They performed experimental tests on the effect of vortex limiter on the cyclone performance. In the area of new design cyclones, some studies have been carried on in recent years. Safikhani and Mehrabian [16] numerically modeled the new design cyclone extracted by Karagoz and investigated the effect of different parameters on the cyclone performance. Safikhani [17] investigated and optimized static new design cyclones with the combination of CFD, neural network and genetic algorithm methods. Safikhani and Allahdadi [18] investigated the effect of magnetic field on new design cyclone performance. Safikhani et al. [19] numerically analyzed the performance of the new design cyclones with more than one inlet. Safikhani and Esmaeili [20] numerically modeled new design dynamic cyclones and showed the impact of different parameters on the performance of new cyclones. Moreover, in recent years, many researchers in the field of flat tubes have provided numerical and experimental research [21-24].
According to the available literature, there is no study on the effect of vortex finder geometry on performance and flow field in new design cyclones. In this paper, the effect of vortex finder shape on the performance and flow field of the new design cyclones is numerically investigated using CFD techniques. Nine different geometries of vortex finder are studied in three categories each with three geometries. In the first category, the effect of vortex finder flattening is investigated. In the second category, vortex finders with three different cross section geometries namely circle, square and triangle are modeled. Finally, in the third category circular vortex finders with three different diameters are modeled.

2 Numerical Modeling

2.1 Geometry

New design of cyclones is grounded on the idea that with lowering frictional hysteresis in cyclones would lead to a climb in vortex length and separation performance.

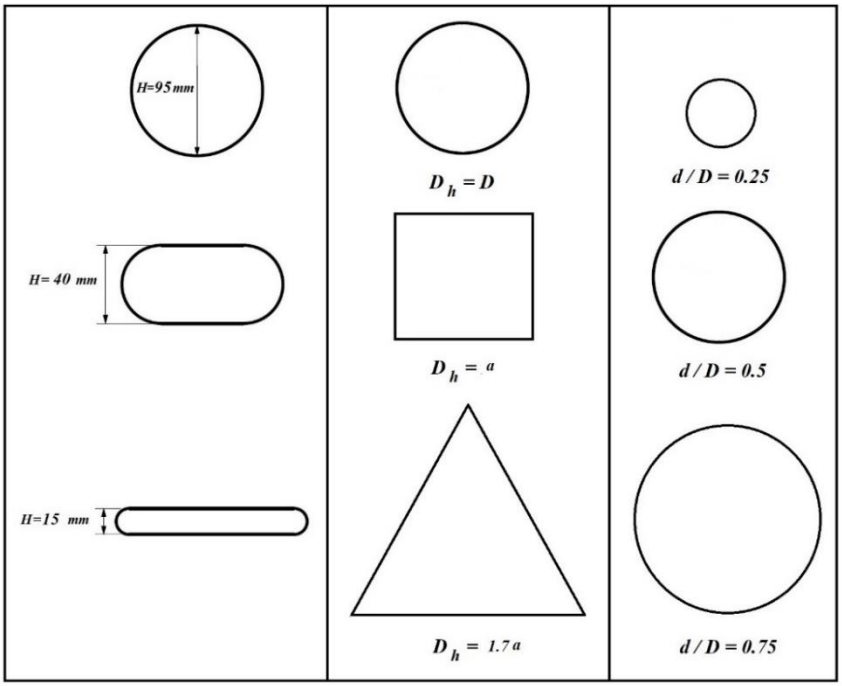

Figure 2 Nine different geometries of vortex finder that are investigated in this paper.

This design remarkably differs from a conventional cyclone in terms of separation space. Such novel cyclone has inner and outer cylinders eliminating the cone and vortex breaker in conventional ones. Flow, tangent to the inner cylinder enters the cyclone where inner cylinder serves as the main frictional surface producing vortex. Then flow, almost frictionless, through outer cylinder helically streams to the bottom of the inner cyclone. After that, facing the impingement surface, flow moves back to the outlet pipe. Location of vortex breaker can be manipulated but ineffective on the length of the vortex. Particles move towards the wall of the outer cylinder and under the influence of centrifugal forces, particles, being separated from the flow, are collected in the bottom of the outer cylinder. This is outer cylinder in where separation occurs. The new design also facilitates simpler manufacturing and lower maintained costs [15]. Fig. (2) shows different geometries of the vortex finder geometry studied in this paper. As can be seen, the first set with three different flattened vortex finders, the second set with circular, square and triangular cross section and the third set three diameters of circular vortex finders are investigated.

2.2 Governing Equations

For an incompressible fluid flow, the equation of continuity and momentum are as follows:

$$\frac{\partial \overline{u}_i}{\partial x_i} = 0 \tag{1}$$

$$\frac{\partial \bar{u}_i}{\partial t} + \overline{u_j}\,\frac{\partial \bar{u}_i}{\partial x_j} = -\frac{1}{\rho}\frac{\partial \bar{P}}{\partial x_i} + \nu\frac{\partial^2 \bar{u}_i}{\partial x_j \partial x_j} - \frac{\partial}{\partial x_j}\,R_{ij} \tag{2}$$

In above equations $\bar{u}_i$ is the velocity, x_i is the position, $\bar{P}$ is the pressure, ρ is the gas density, ν is the kinematic viscous and $R_{ij} = \overline{u'_\iota u_j{}'}$ is the Reynolds stress tensor. Here, $u'_i = u_i - \overline{u_\iota}$ is the ith fluctuating velocity.

The RSTM calculates differential transport equations for evaluation of the turbulence stress components where the turbulence production terms are as follows:

$$\begin{aligned}\frac{\partial}{\partial t}R_{ij} + \overline{u_k}\,\frac{\partial}{\partial x_k}R_{ij} = \frac{\partial}{\partial x_k}\left(\frac{\nu_t}{\sigma^k}\frac{\partial}{\partial x_k}R_{ij}\right) - \left[R_{ik}\frac{\partial \overline{u_j}}{\partial x_k} + R_{jk}\frac{\partial \bar{u}_i}{\partial x_k}\right] \\ - C_1\frac{\varepsilon}{K}\left[R_{ij} - \frac{2}{3}\delta_{ij}K\right] - C_2\left[P_{ij} - \frac{2}{3}\delta_{ij}P\right] - \frac{2}{3}\delta_{ij}\varepsilon\end{aligned} \tag{3}$$

$$P_{ij} = -\left[R_{ik}\frac{\partial \bar{u}_j}{\partial x_k} + R_{jk}\frac{\partial \bar{u}_i}{\partial x_k}\right], P = \frac{1}{2}P_{ij} \tag{4}$$

With P being the fluctuating kinetic energy production. ν_t is the turbulent (eddy) viscosity; and $\sigma^k = 1$, $C_1 = 1.8$, $C_2 = 0.6$ are empirical constants [25].

The transport equation for the turbulence dissipation rate, ε, is as follows:

$$\frac{\partial \varepsilon}{\partial t} + \overline{u_j}\,\frac{\partial \varepsilon}{\partial x_j} = \frac{\partial}{\partial x_j}\left[\left(\nu + \frac{\nu_t}{\sigma^\varepsilon}\right)\frac{\partial \varepsilon}{\partial x_j}\right] - C^{\varepsilon 1}\frac{\varepsilon}{K}R_{ij}\frac{\partial \bar{u}_i}{\partial x_j} - C^{\varepsilon 2}\frac{\varepsilon^2}{K} \tag{5}$$

In Eq. (5), $K = \frac{1}{2}\overline{u'_\iota u_\iota{}'}$ is the fluctuating kinetic energy, and ε is the turbulence dissipation rate. The values of constants are $\sigma^{\varepsilon} = 1.3, C^{\varepsilon 1} = 1.44 \ and \ C^{\varepsilon 2} = 1.92$.
The dispersion of small particles is generally affected by the fluctuation of momentum. The turbulence fluctuations are random functions of position and time. In this study, a discrete random walk (DRW) model is used for evaluating the velocity fluctuations. The values of u', v' and w' that prevail during the lifetime of the turbulent eddy, T_e are sampled by assuming that they obey a Gaussian probability distribution. In this model the velocity in the ith direction is given as:

$$u_i' = \xi\sqrt{\overline{u_i' u_i'}} \tag{6}$$

In Eq. (6), ξ is a zero-mean, unit-variance, normally distributed random number, $\sqrt{\overline{u_i' u_i'}}$ is the local root mean-square (RMS) fluctuation velocity in the ith direction , and the summation convention on i is suspended.
The characteristic lifetime of the eddy is defined as a constant given by:

$$T_e = 2T_l \tag{7}$$

Where, T_l is the eddy turn over time given as, $T_e = 0.3\ \frac{K}{\varepsilon}$ in the RSTM. The other option allows for a long –normal random variation of eddy lifetime that is given by:

$$T_e = -T_l \log r \tag{8}$$

Where, r is a uniform random number between 0 and 1. The particle is assumed to interact with the fluid fluctuation field, which stays fixed over the eddy lifetime. When the eddy lifetime is reached, a new value of the instantaneous velocity is obtained by introducing a new value of ξ in Eq. (6).
There are two main methods for modeling multiphase flows that account for the interactions between the phases. These are the Eulerian and the Lagrangian approaches. The former is based on the concept of interpenetrating continua, for which all the phases are investigated as continuous media with properties analogous to those of a fluid. The Lagrangian approach adopts a continuum description for the fluid phase and tracks the discrete phase using Lagrangian particle trajectory analysis.
In the present study, one way coupling approach is used to solve the two phase flow and the Lagrangian approach is implemented for simulation of second discrete phase (particles) using FLUENT. In this model, air is the continuous phase and the particles are treated as the dispersed discrete phase. The volume-averaged and steady state momentum equation is solved for the gas phase. The particle motions are simulated by the Lagrangian method. Forces acting on the dispersed phase include drag and gravity. The discrete phase equations are solved using Runge-Kutta method for particles.
To calculate the trajectories of particles in the flow, the discrete phase model (DPM) is used to track individual particles through the continuum fluid. The particle loading in a cyclone separator is typically small, and therefore, it can be safely assumed that the presence of the particles does not affect the flow field (one-way coupling method).
The equation of motion of small particles, including the effect of nonlinear drag and gravitational forces, is given by:

$$\frac{du_i^p}{dt} = \frac{3vC_D Re_p}{4d^2 S}\left(u_i - u_p^i\right) + g_i \tag{9}$$

$$\frac{dx_i}{dt} = u_i^p \tag{10}$$

Here, u_i^p is the velocity of the particle and x_i is its position, d is the particle diameter, S is the ratio of particle density to fluid density, and g_i is the acceleration of gravity. The term on the right hand side of Eq. (10) is the drag force due to the relative slip between the particle and the fluid. The drag force is, generally, the dominating force. According to [26], the drag coefficient, C_D is as follows:

$$C_D = \frac{24}{Re_p} \quad \text{for } Re_p < 1 \tag{11}$$

$$C_D = \frac{24}{Re_p}\left(1 + \frac{1}{6}{Re_p}^{\frac{2}{3}}\right) \quad \text{for} \quad 1 < Re_p < 400 \tag{12}$$

Where Re_p is the particle Reynolds number defined as:

$$Re_p = \frac{\left|u_j - u_j^p\right| d}{\nu} \tag{13}$$

The particle equation of motion requires the instantaneous turbulent fluid velocity values at particle locations. The mean liquid velocity was evaluated by the use of the Reynolds stress transport turbulence model (RSTM) and the fluctuation velocity components were calculated from Eq. (6). The drag coefficient for spherical particles is calculated by using the correlations investigated by Morsi and Alexander [27]. The ordinary differential equation (Eq. (10)) is integrated along the trajectory of a particle.

Collection efficiency values are obtained by releasing a specified number of mono-dispersed particles at the inlet of the cyclone and by monitoring the number escaping through the underflow. The more particles are tracked in cyclones, the higher the accuracy of collection efficiency will be. The collision between the particles and the cyclone wall was considered a complete elastic one with restitution coefficient of 0.8 [13]. Moreover the collisions between particles are neglected. Selection of time step plays a role in convergence; if large values are chosen simulation is likely to diverge and if it is too small computation time exponentially increases. For steady state problems, false time step of 0.2 ms is used for tracking the particles in numerical model. The false time steps used in the simulations are shown in Table (1).

Table 1 False time steps used for the simulation.

Parameters	False time step
Pressure	0.2
u (x-velocity)	0.4
v (y-velocity)	0.4
w (z-velocity)	0.4
k (turbulent kinetic energy)	0.5
ε (turbulent dissipation rate)	0.5
Reynolds stresses	0.5

2.3 Numerical methods

In the present simulations, the finite volume methods have been used to discrete the partial differential equations of the model using the SIMPLE method for pressure–velocity coupling and the second-order upwind scheme to interpolate the variables on the surface of the control volume. The RSTM is used in the simulation, and the computation is continued until the solution converged with a total relative error of less than 0.00001. The velocity inlet boundary condition is used at the inlet. The pressure outlet boundary condition is used at the outlet. Some operating conditions in simulations are shown in Table (2).
To attain confidence that the obtained results are independent of the size and the number of generated grids, several grids with different sizes has been tested for each cyclone; and it has been attempted to consider for each cyclone the best grid, with the highest accuracy and the lowest computation cost. A number of 900,000–1,100,000 hexahedral cells are generated for solving the flow field in the new cyclones. Fig. (3) shows a sample of grid generation for new design cyclones.

Table 2 Operating conditions in numerical simulations.

Parameter	Values
Inlet velocity (m/s)	10
Particle feed rate (g/min)	15
Particle density (kg/m^3)	2000
Inlet temperature (K)	300

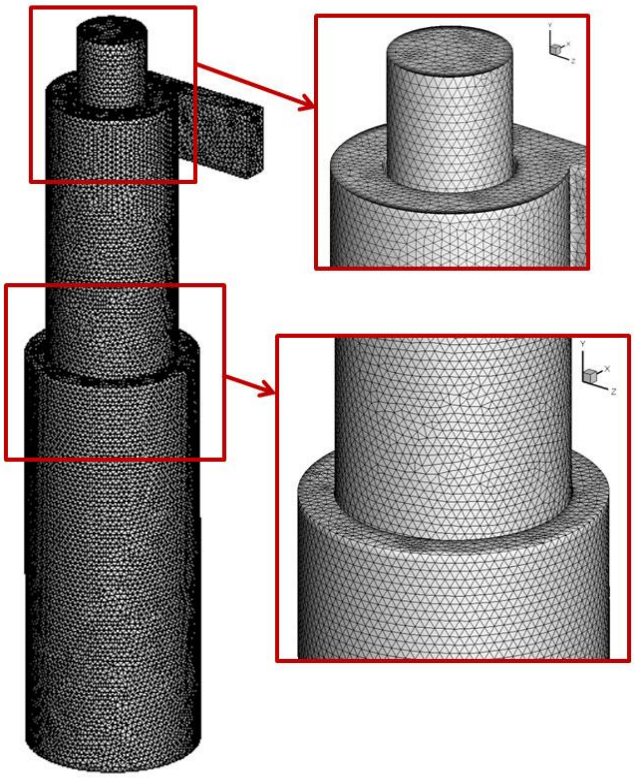

Figure 3 A sample of generated grid for numerical study of new cyclones.

2.4 Validation

To attain the confidence about the simulations, it is necessary to compare the numerical results with the available numerical or experimental data. The comparison between experimental, analytical Wang model and the present numerical results for pressure drop as a function of inlet velocity is shown in Fig. (4) for conventional cyclones. As is evident from this figure the present simulations agree well with the available experimental and analytical data. For validating the collection efficiency results, Table (3) compares the present numerical results and the related experimental data of Wang [28] for different PSDs in conventional cyclones. In Table (3), D_{50} is the diameter of a particle which has 50% probability of separation and 50% probability of escaping and is a criterion for comparing efficiency of cyclones. Physical characteristics of *A*–*E* particles are shown in the Table (3). *MMD* and *GSD* are Mass Median Diameter and Geometric Standard Deviation, respectively. As shown in this table a good agreement is observed between numerical simulations and experimental results.

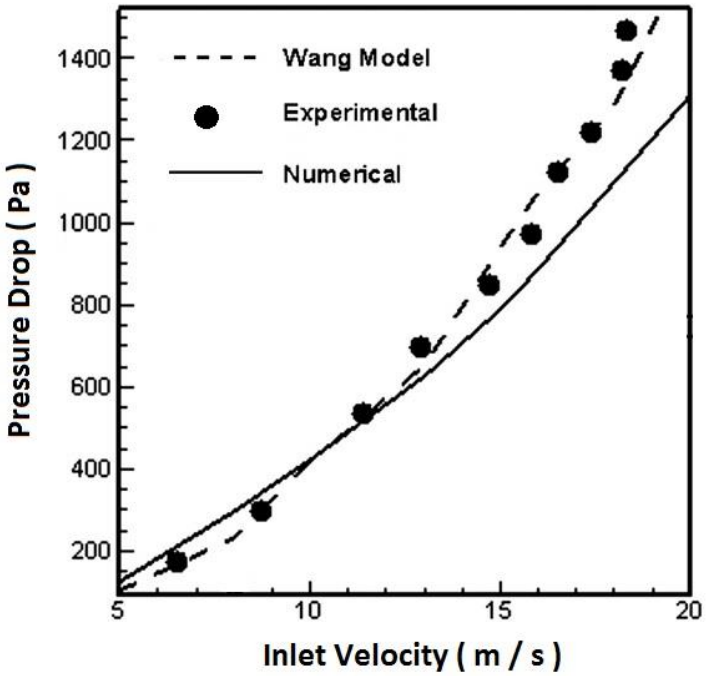

Figure 4 Comparison of numerical, experimental [28] and analytical result for pressure drop (Pa)

Table 3 Comparison of numerical, theoretical and experimental D_{50}

Dust	*PSD*		D_{50}	
	ρ_P	*MMD/GSD*	Experimental	Numerical
A	1.77	20/2	2.74	2.41
B	1.82	21/1.9	3.75	3.32
C	1.87	23/1.8	3.60	3.151
D	1.52	19/1.4	-	7.1
E	2.73	13/1.7	4.40	4.07

3 Results and discussion

In this paper, the effect of vortex finder shape on the performance and flow field of the new design cyclones is numerically investigated using CFD techniques. Nine different geometries of vortex finder as shown in Fig. (2) are studied in three categories each with three geometries. In the first category, the effect of vortex finder flattening is investigated. In the second category, vortex finders with three different cross section geometries namely circle, square and triangle are modeled. Finally, in the third category circular vortex finders with three different diameters are modeled.

The investigated particle diameters are between 0.1 μm and 134 μm. The cumulative particle size distribution (PSD) is shown in Fig. (5). For applying this PSD in numerical simulation the Rosin-Rammler method is used. The Rosin-Rammler distribution function is based on the assumption that an exponential relationship exists between the particle diameter, d, and the fraction of particles with diameter greater than d, Y_d:

$$Y_d = e^{-(d/\bar{d})^n} \tag{14}$$

Where $\bar{d}$ is the mean diameter in PSD and can be calculated as the diameter at which $Y_d = e^{-1} \approx 0.368$. Similarly, n is the spread diameter and can be calculated as the follows:

$$n = \frac{ln(-\ln Y_d)}{ln(d/\bar{d})} \tag{15}$$

In this paper, $\bar{d}$ and n are calculated as 44.4 μm and 1.68, respectively. Using the mentioned method, the collection efficiency in the new design cyclone separators with different vortes finder shape is calculated.

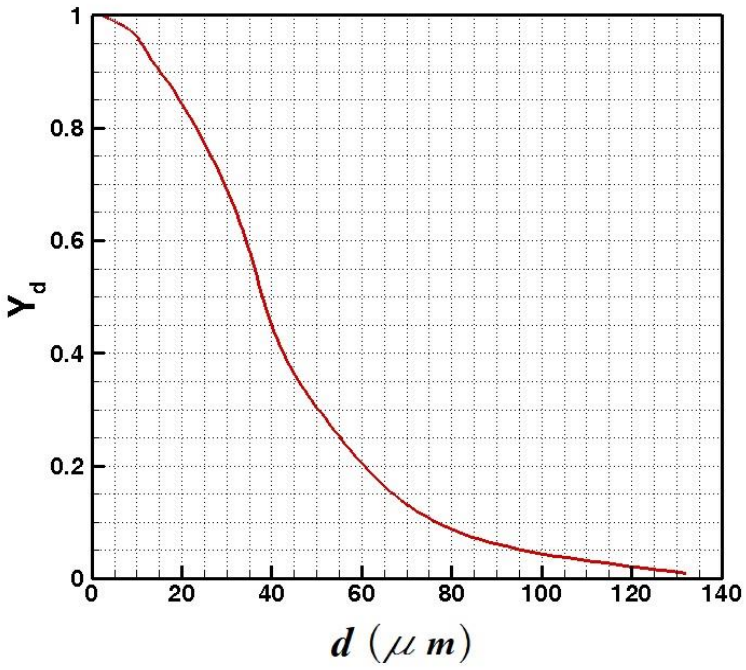

Figure 5 Cumulative particle size distributions investigated in the present study.

Fig. (6) shows the effect of the vortex finder flattening on the collection efficiency and pressure drop of the new design cyclones in different inlet velocities. As can be seen, with higher inlet velocities, the efficiency and pressure drop remarkably increase in all three flattening. In all range of inlet velocities, the circular tube has maximum efficiency and minimum pressure drop. Flattening the vortex finder causes lower efficiency and higher pressure drop. So, using flattened vortex finder is totally rejected. It should be noted that the periphery of three flattened vortex finder are equal because it reflects the manufacturing process of such tubes in which they are compressed by two parallel plates on their periphery. Therefore, their periphery remains constant and equal to circular one.

Velocity distribution is directly correlated with the separation efficiency of cyclones. Figs. (7) and (8) illustrate axial velocity contour, turbulence energy, velocity vectors and trajectory the particles in three vortex finder flattening. These figures can define the flow field in new design vortex finder with different flattening. As shown, with increasing the flattening, a severe accumulating the particles and hence a severe turbulence in the inlet of the vortex finder occurs and lowers the efficiency. Similarly, tracking the particles in Fig. (8) shows that flow field constituting a vortex in the center of the cyclone is normally shaped.

Pressure drop between inlet and outlet is one of the important objective functions in cyclones. Many empirical models have been proposed for the pressure drop in the cyclones [28]. In Wang's model the total pressure drop in the cyclone is obtained by summing the five pressure drop components as follows:

$$\Delta P_{total} = \Delta P_e + \Delta P_k + \Delta P_f + \Delta P_r + \Delta P_e \Delta P_o \tag{16}$$

Where, the components of Eq. (16) are explained in Table (4). Fig. (9) shows pressure distribution in new design cyclones with flattened vortex finders. Lower pressure values in the center of cyclones for all cases are attributed to the effect of the tangent velocity which is unanimously known. As can be seen, vortex finder which is highly flattened possesses remarkable pressure drop which is not favorable.

Fig. (10) compares the performance of new design cyclones with vortex finders of different circular, square and triangular cross section. In this figure, the efficiency pertained to the triangular cross section is not illustrated. This is because in vortex finder with triangular cross section, the sharp edge of the vortex finder places on the path of the flow and vortex is not formed properly. Therefore, the mixture of the fluid and particles, without the presence of a vortex, move to the bottom of the cyclone and the performance is detrimentally affected. Thus triangular-sectioned vortex finders by no mean are appropriate. Among other two cross sections, according to Fig. (10), circular cross section, in all inlet velocities, has the highest efficiency albeit with the highest pressure drop. The lowest pressure drop occurred in triangular vortex finder and then square one.

Figs. (11) and (12) illustrate axial velocity contour, turbulence kinetic energy, velocity vectors and trajectory the particles in three vortex finder shapes. These figures can define the flow field in new design vortex finder with different shapes. Lack of vortex formation and improper functioning of the cyclone in the triangular vortex finder is well evident in all the above figures. Fig. (13) shows pressure distribution in new design cyclones with different vortex finder shapes. Lower pressure values in the center of cyclones for all cases are attributed to the effect of the tangent velocity which is unanimously known. It should be noted that all the three vortex finder shapes studied in this paper have the same hydraulic diameter.

Finally, Fig. (14) shows the effect of vortex finder diameter on the performance of new design cyclones. As it turns out, as the diameter of the vortex finder increases, the efficiency worsens (decreases) and the pressure drop improves (decreases). The presented study can be utilized to design new design cyclones with superior performance.

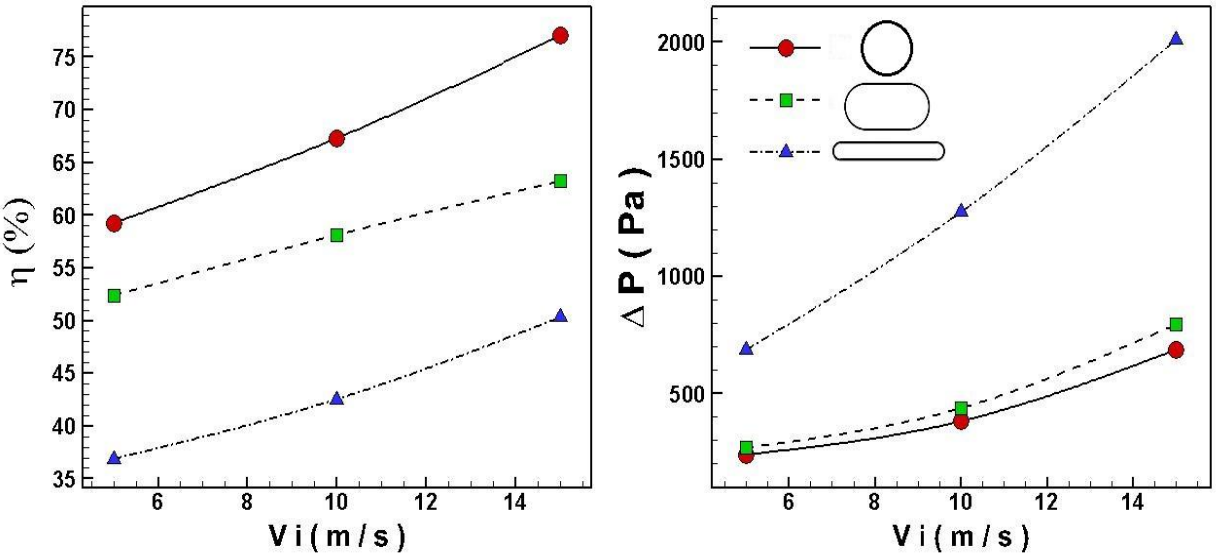

Figure 6 Effect of vortex finder flattening and inlet velocity on new design cyclone performance: collection efficiency (left) Pressure drop (right).

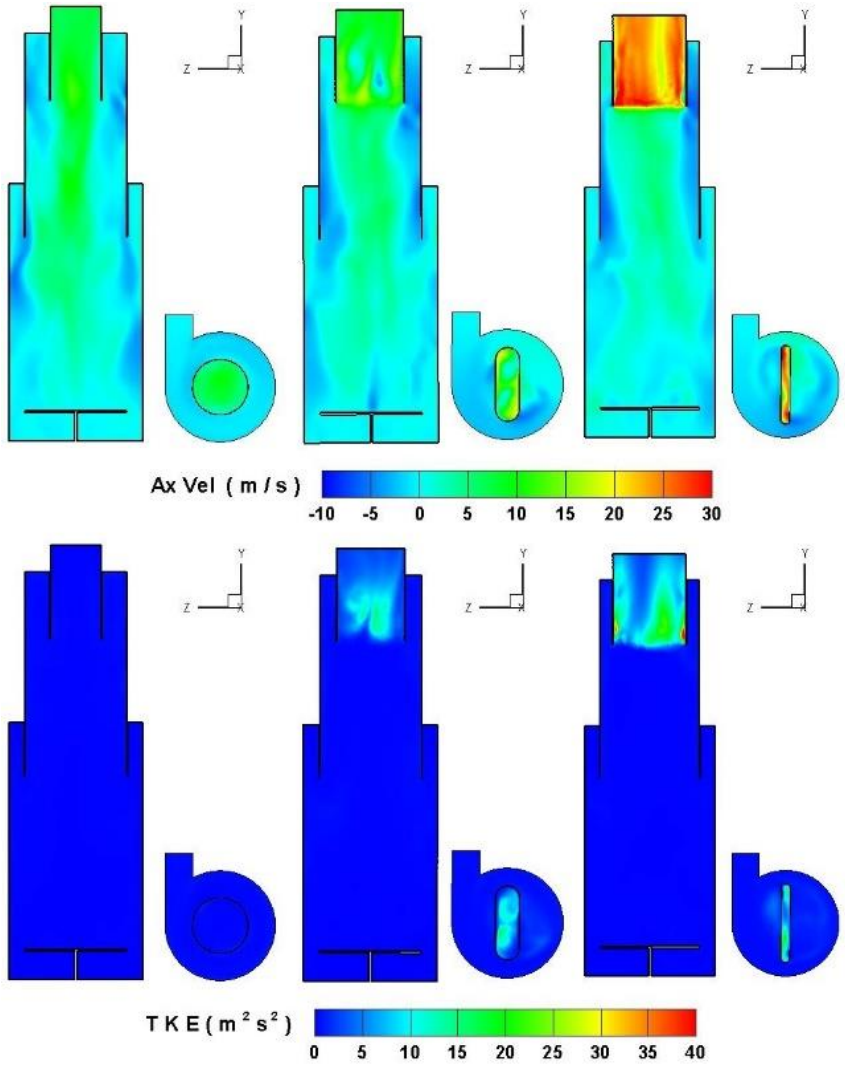

Figure 7 Axial velocity (top) and turbulent kinetic energy (bottom) distribution contours at the middle plane of new design cyclones with different vortex finder flattening.

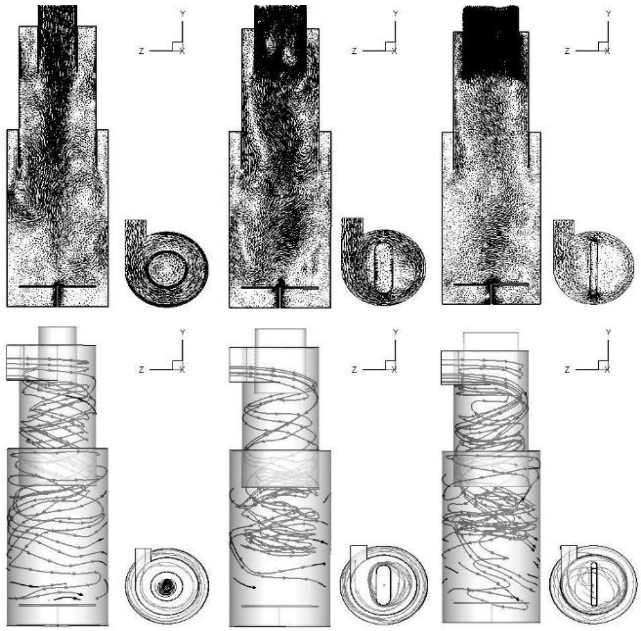

Figure 8 Velocity vectors (top) and particle trajectory (bottom) in new design cyclones with different vortex finder flattening.

Table 4 The components of Wang's pressure drop theory.

Components	Definition
$\Delta P_e = C_2 VP_{in}$	Entry loss, $C_2 \approx 1$, VP = Velocity pressure
$\Delta P_k = VP_{in} - VP_{out}$	Kinetic energy loss
$\Delta P_f = CVP_{in}$	Frictional loss, $C_{1D3D} = 0.14$, $C_{2D2D} = 0.28$, $C_{1D2D} = 0.15$
$\Delta P_r = \rho V_{in}^2 (R/r_0 - 1)$	Rotational loss, r_0 = radius of the vortex interface, R = cyclone body radius
$\Delta P_0 = C_3 VP_{out}$	Pressure loss in the inner vortex and exit tube, $C_3 \approx 1.8$

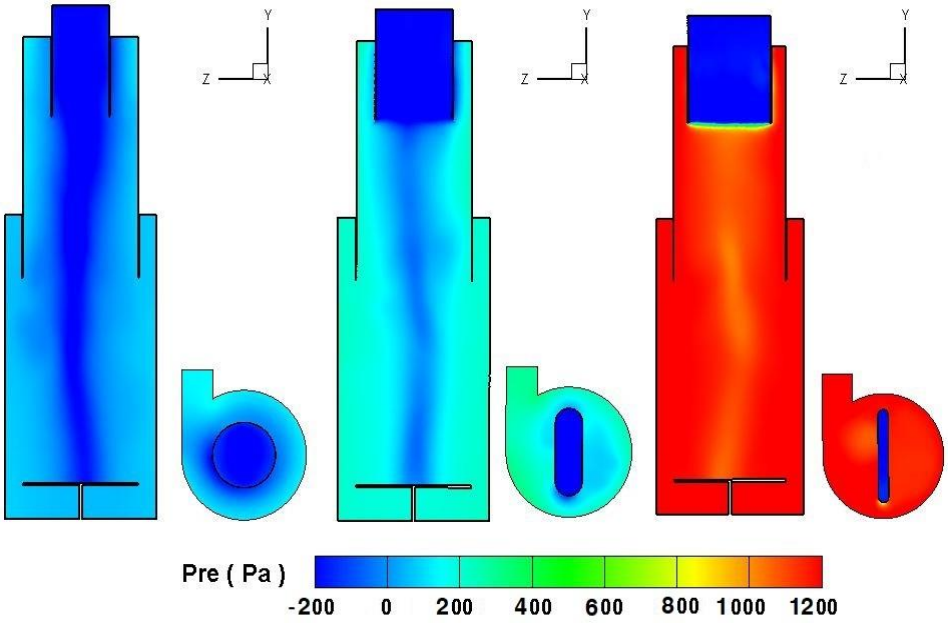

Figure 9 Pressure distribution contours at the middle plane of new design cyclones with different vortex finder flattening.

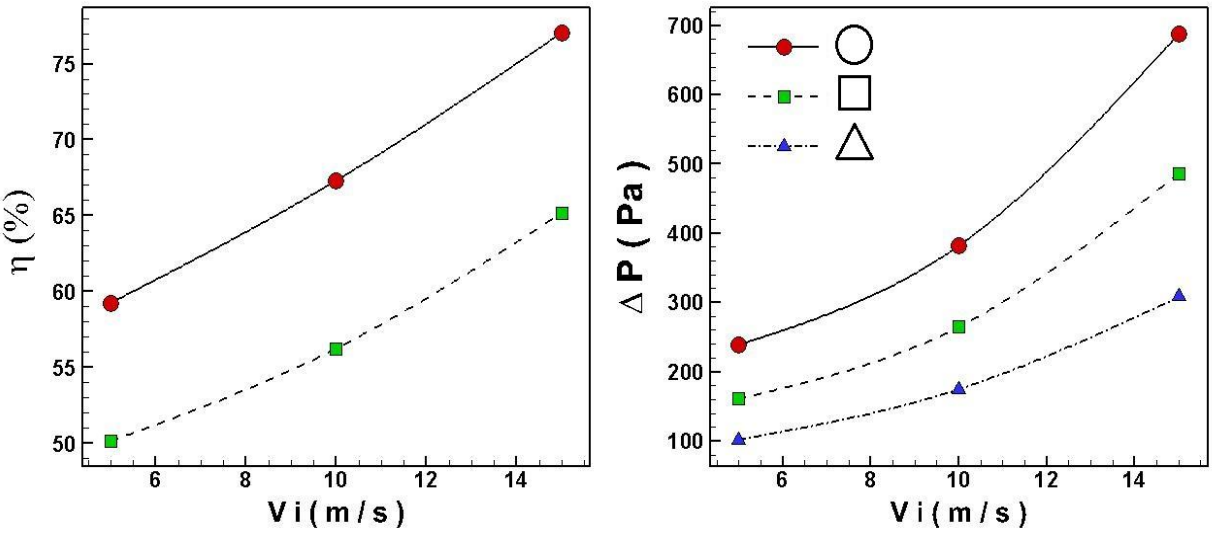

Figure 10 Effect of vortex finder shape and inlet velocity on new design cyclone performance: collection efficiency (left) Pressure drop (right).

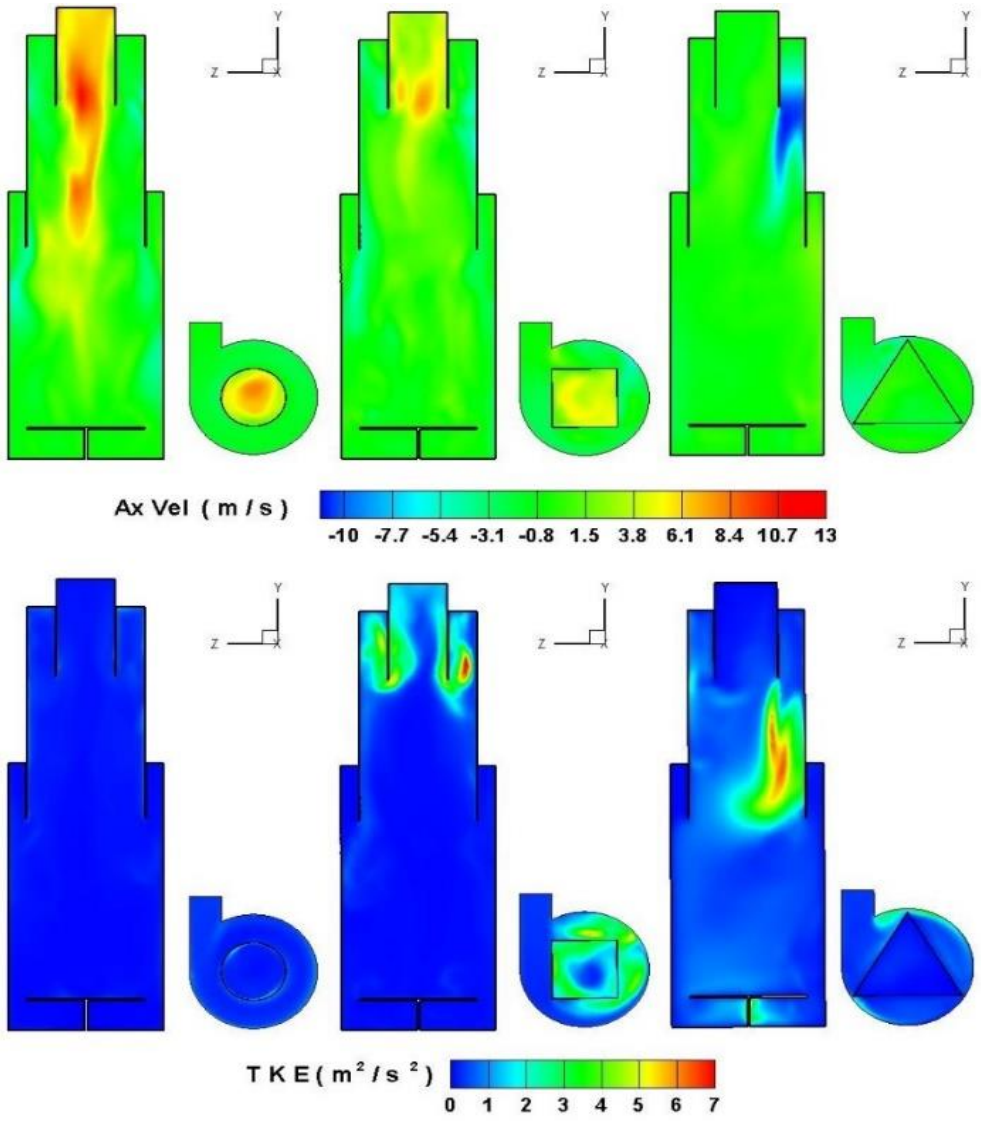

Figure 11 Axial velocity (top) and turbulent kinetic energy (bottom) distribution contours at the middle plane of new design cyclones with different vortex finder shape.

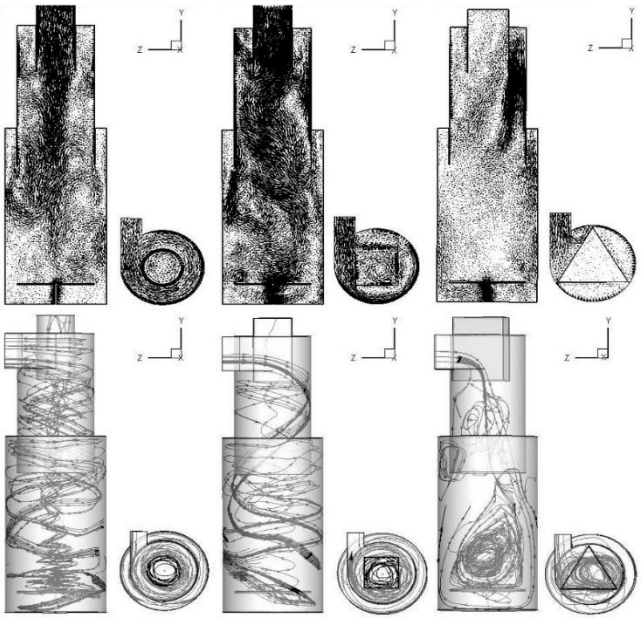

Figure 12 Velocity vectors (top) and particle trajectory (bottom) in new design cyclones with different vortex finder shape.

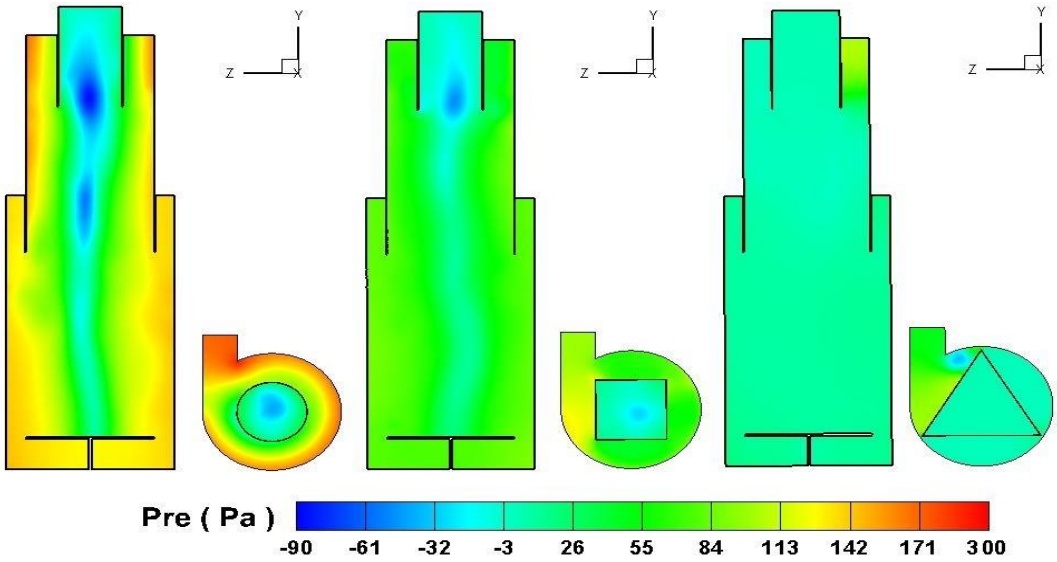

Figure 13 Pressure distribution contours at the middle plane of new design cyclones with different vortex finder shape.

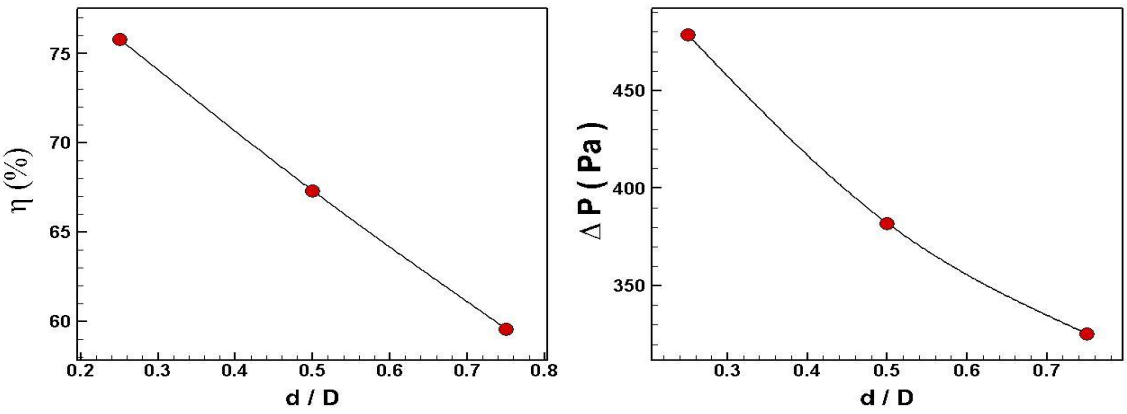

Figure 14 Effect of vortex finder diameter and inlet velocity on new design cyclone performance: collection efficiency (left) Pressure drop (right).

4 Conclusion

In this paper, the effect of vortex finder shape on the performance and flow field of the new design cyclones was numerically investigated using CFD techniques. Nine different geometries of vortex finder were studied in three categories each with three geometries. In the first category, the effect of vortex finder flattening was investigated. In the second category, vortex finders with three different cross section geometries namely circle, square and triangle were modeled. Finally, in the third category circular vortex finders with three different diameters were modeled. The new design cyclone was based on the idea of improving cyclone collection efficiency and pressure drop by increasing the vortex length. The Reynolds averaged Navier–Stokes equations with Reynolds stress turbulence model (RSM) were solved. The Eulerian-Lagrangian computational procedure was used to predict particles tracking in the cyclones. The velocity fluctuations were simulated using the Discrete Random Walk (DRW).
The results show that in the flat category, vortex finder without flattening (circular cross section) possess the maximum efficiency and the lowest pressure drop and with flattening, the cyclone efficiency dramatically decreases while pressure drop remarkably increases. So, using flattened vortex finder is totally rejected. With increasing the flattening, a severe accumulating the particles and hence a severe turbulence in the inlet of the vortex finder occurs and lowers the efficiency. Among the vortex finder with different cross section, maximum efficiency is associated to the circular vortex finder while the lowest pressure drop is assigned to the triangle one. In vortex finder with triangular cross section, the sharp edge of the vortex finder places on the path of the flow and vortex is not formed properly. Therefore, the mixture of the fluid and particles, without the presence of a vortex, move to the bottom of the cyclone and the performance is detrimentally affected. Thus triangular-sectioned vortex finders by no mean are appropriate. Finally, as the diameter of the vortex finder increases, the efficiency worsens (decreases) and the pressure drop improves (decreases). The presented study can be utilized to design new design cyclones with superior performance.

Ethical statement:

- **Funding**: The authors did not receive support from any organization for the submitted work.

- **Conflict of interest:** The authors of this paper certify that they have NO affiliations with or involvement in any organization or entity with any financial interest (such as honoraria; educational grants; participation in speakers' bureaus; membership, employment, consultancies, stock ownership, or other equity interest; and expert testimony or patent-licensing arrangements), or non-financial interest (such as personal or professional relationships, affiliations, knowledge or beliefs) in the subject matter or materials discussed in this manuscript.

- **Ethical approval**: This material is the authors' own original work, which has not been previously published elsewhere. The paper is not currently being considered for publication elsewhere. The paper reflects the authors' own research and analysis in a truthful and complete manner. The paper properly credits the meaningful contributions of co-authors. The results are appropriately placed in the context of prior and existing research. All sources used are properly disclosed. All authors have been personally and actively involved in substantial work leading to the paper, and will take public responsibility for its content.

- **Informed consent:** No applicable.

References

[1] Alexander, R.M., "Fundamentals of Cyclone Design and Operation", Proceedings Australian Institute of Minerals Metals, Vol. 152, pp. 203–228, (1949).

[2] Elsayed, K., and Lacor, C., "The Effect of Cyclone Inlet Dimensions on the Flow Pattern and Performance", Applied Mathematical Modelling, Vol. 35, pp. 1952–1968, (2011).

[3] Zhao, B., Su, Y., and Zhang, J., "Simulation of Gas Flow Pattern and Separation Efficiency in Cyclone with Conventional Single and Spiral Double Inlet Configuration", Chemical Engineering Research and Design, Vol. 84, pp. 1158–1165, (2006).

[4] Xiang, R.B., and Lee, K.W., "Exploratory Study on Cyclones of Modified Designs", Particulate Science and Technology, Vol. 19, pp. 327–338, (2001).

[5] Chuah, T.G., Gimbun, J., and Choong, T.S.Y., "A CFD Study of the Effect of Cone Dimensions on Sampling Aerocyclones Performance and Hydrodynamics", Powder Technology, Vol. 162, pp. 126–132, (2006).

[6] Xiang, R., Park, S.H., and Lee, K.W., "Effects on Cone Dimension on Cyclone Performance", Journal of Aerosol Science, Vol. 32, pp. 549–561, (2011).

[7] Yoshida, H., Fukui, K., Yoshida, K., and Shinoda, E., "Particle Separation by Iinoya's Type Gas Cyclone", Powder Technology, Vol. 118, pp. 16–23, (2001).

[8] Qian, F., Zhang, J., and Zhang, M., "Effects of the Prolonged Vertical Tube on the Separation Performance of a Cyclone", Journal of Hazardous Material, Vol. 136, pp. 822–829, (2006).

[9] Kaya, F., and Karagoz, I., "Numerical Investigation of Performance Characteristics of a Cyclone Prolonged with a Dipleg", Chemical Engineering Journal, Vol. 151, pp. 39–45, (2009).

[10] Yoshida, H., Akiyama, S., Fukui, K., and Taniguchi, S., "Effect of Apex Cone Height on Particle Classification Performance of a Cyclone Separator", Advanced Powder Technology, Vol. 14, No. 3, pp. 263–278, (2003).

[11] Yoshida, H., Nishimura, Y., Fukui, K., and Yamamoto, T., "Effect of Apex Cone Shape on Fine Particle Classification of Gas-cyclone", Powder Technology, Vol. 204, pp. 54–62, (2010).

[12] Kepa, A., "The Effect of a Counter-cone Position on Cyclone Performance", Separation Science and Technology, Vol. 47, pp. 2250–2255, (2012).

[13] Khalkhali, A., and Safikhani, H., "Pareto Based Multi-objective Optimization of a Cyclone Vortex Finder using CFD, GMDH Type Neural Networks and Genetic Algorithms", Engineering Optimization, Vol. 44, No. 1, pp. 105-118, (2012).

[14] Raoufi, A., Shams, M., Farzaneh, M., and Ebrahimi, R., "Numerical Simulation and Optimization of Fluid Flow in Cyclone Vortex Finder", Chemical Engineering Process, Vol. 47, pp. 128–137, (2008).

[15] Karagoz, I., Atakan, A., Surmen, A., and Sendogan, O., "Design and Performance Evaluation of a New Cyclone Separator", Journal of Aerosol Science, Vol. 59, pp. 57–64, (2013).

[16] Safikhani, H., and Mehrabian, P., "Numerical Study of Flow Field in New Cyclone Separators", Advanced Powder Technology, Vol. 27, pp. 379–387, (2016).

[17] Safikhani, H., "Modeling and Multi-objective Pareto Optimization of New Cyclone Separators using CFD, ANNs and NSGA II Algorithm", Advanced Powder Technology, Vol. 27, pp. 2277–2284, (2016).

[18] Safikhani, H., and Allahdadi, S., "The Effect of Magnetic Field on the Performance of New Design Cyclone Separators", Advanced Powder Technology, Vol. 31, pp. 2541–2554, (2020).

[19] Safikhani, H., Zamani, J., and Musa, M., "Numerical Study of Flow Field in New Design Cyclone Separators with One, Two and Three Tangential Inlets", Advanced Powder Technology, Vol. 29, pp. 611–622, (2018).

[20] Safikhani, H., Esmaeili, F., and Salehfard, S., "Numerical Study of Flow Field in New Design Dynamic Cyclone Separators", International Journal of Engineering Transactions B: Applications, Vol. 33, No. 2, pp. 357-365, (2020).

[21] Wilson, M.J., Newell T.A., Chato, J.C., and Ferreira, C.A.I., "Refrigerant Charge, Pressure Drop and Condensation Heat Transfer in Flattened Tubes", International Journal of Refrigeration, Vol. 26, pp. 442–451, (2003).

[22] Quiben, J., Cheng, L., da Silva, J., and Thome, J.R., "Flow Boiling in Horizontal Flattened Tubes: Part I – Two-phase Frictional Pressure Drop Results and Model", International Journal of Heat and Mass Transfer, Vol. 52, pp. 3645–3653, (2009).

[23] Nasr, M., Akhavan-Behabadi, M.A., and Marashi, S.E., "Performance Evaluation of Flattened Tube in Boiling Heat Transfer Enhancement and its Effect on Pressure Drop", International Communication in Heat and Mass Transfer, Vol. 37, pp. 430–436, (2010).

[24] Safikhani, H., and Abbassi, A., "Effects of Tube Flattening on the Fluid Dynamic and Heat Transfer Performance of Nanofluids", Advanced Powder Technology, Vol. 25, pp. 1132–1141, (2014).

[25] Launder, B.E., Reece, G.J., and Rodi, W., "Progress in the Development of a Reynolds Stress Turbulent Closure", Journal of Fluid Mechanics, Vol. 68, pp. 537–538, (1975).

[26] Hinds, W.C., "*Aerosol Technology, Properties Behavior and Measurement of Airborne Particles*", John Wiley and Sons, New York, Third Edition, (1982).

[27] Morsi, S.A., and Alexander, A.J., "An Investigation of Particle Trajectories in Two Phase Flow Systems", Journal of Fluid Mechanics, Vol. 55, pp. 193–208, (1972).

[28] Wang, L., "Theoretical Study of Cyclone Design", Ph.D. Thesis, Texas A&M University, USA, (2004).